

Unphysical Discontinuities in GW Methods

Mickaël Vérit,¹ Pina Romaniello,^{2,3} J. A. Berger,^{1,3} and Pierre-François Loos^{1, a)}

¹⁾*Laboratoire de Chimie et Physique Quantiques, Université de Toulouse, CNRS, UPS, France*

²⁾*Laboratoire de Physique Théorique, Université de Toulouse, CNRS, UPS, France*

³⁾*European Theoretical Spectroscopy Facility (ETSF)*

We report unphysical irregularities and discontinuities in some key experimentally-measurable quantities computed within the GW approximation of many-body perturbation theory applied to molecular systems. In particular, we show that the solution obtained with partially self-consistent GW schemes depends on the algorithm one uses to solve self-consistently the quasi-particle (QP) equation. The main observation of the present study is that each branch of the self-energy is associated with a distinct QP solution, and that each switch between solutions implies a significant discontinuity in the quasiparticle energy as a function of the internuclear distance. Moreover, we clearly observe “ripple” effects, i.e., a discontinuity in one of the QP energies induces (smaller) discontinuities in the other QP energies. Going from one branch to another implies a transfer of weight between two solutions of the QP equation. The case of occupied, virtual and frontier orbitals are separately discussed on distinct diatomics. In particular, we show that multisolution behavior in frontier orbitals is more likely if the HOMO-LUMO gap is small.

I. BACKGROUND

Many-body perturbation theory methods based on the one-body Green function G are fascinating as they are able to transform an unsolvable many-electron problem into a set of non-linear one-electron equations, thanks to the introduction of an effective potential Σ , the self-energy. Electron correlation is explicitly incorporated via a sequence of self-consistent steps connected by Hedin’s equations.¹ In particular, Hedin’s approach uses a dynamically screened Coulomb interaction W instead of the standard bare Coulomb interaction. Important experimental properties such as ionization potentials, electron affinities as well as spectral functions, which are related to direct and inverse photo-emission, can be obtained directly from the one-body Green function.² A particularly successful and practical approximation to Hedin’s equations is the so-called GW approximation^{2–4} which bypasses the calculation of the most complicated part of Hedin’s equations, the vertex function.¹

Although (perturbative) G_0W_0 is probably the simplest and most widely used GW variant,^{5–10} its starting point dependence has motivated the development of partially^{11–19} and fully^{20–28} self-consistent versions in order to reduce or remove this undesirable feature. Here, we will focus our attention on partially self-consistent schemes as they have demonstrated comparable accuracy and are computationally lighter than the fully self-consistent version.²⁹ Moreover, they are routinely employed for solid-state and molecular calculations and are available in various computational packages.^{6,13,19,29–34} Recently, an ever-increasing number of successful applications of partially self-consistent GW methods have sprung in the physics and chemistry literature for molecular systems,^{7–10,18,27,30,31,35–41} as well as extensive and elaborate benchmark sets.^{9,10,34,35,42–46}

There exist two main types of partially self-consistent GW methods: i) “eigenvalue-only quasiparticle” GW (evGW),^{11–14} where the quasiparticle (QP) energies are updated at each iter-

ation, and ii) “quasiparticle self-consistent” GW (qsGW),^{15–19} where one updates both the QP energies and the corresponding orbitals. Note that a starting point dependence remains in evGW as the orbitals are not self-consistently optimized in this case.

In a recent article,⁴⁷ while studying a model two-electron system,^{48–53} we have observed that, within partially self-consistent GW (such as evGW and qsGW), one can observe, in the weakly correlated regime, (unphysical) discontinuities in the energy surfaces of several key quantities (ionization potential, electron affinity, HOMO-LUMO gap, total and correlation energies, as well as vertical excitation energies). In the present manuscript, we provide further evidences and explanations of this undesirable feature in real molecular systems. For sake of simplicity, the present study is based on simple closed-shell diatomics (H_2 , F_2 and BeO). However, the same phenomenon can be observed in many other molecular systems, such as LiF , HeH^+ , LiH , BN , O_3 , etc. Although we mainly focus on G_0W_0 and evGW, similar observations can be made in the case of qsGW and second-order Green function (GF2) methods.^{47,54–64} Unless otherwise stated, all calculations have been performed with our locally-developed GW software, which closely follows the MOLGW implementation.³¹

II. THEORY

Here, we provide brief details about the main equations and quantities behind G_0W_0 and evGW considering a (restricted) Hartree-Fock (HF) starting point.⁵⁴ More details can be found, for example, in Refs. 6, 19, and 31.

For a given (occupied or virtual) orbital p , the correlation part of the self-energy,

$$\Sigma_p^c(\omega) = \Sigma_p^p(\omega) + \Sigma_p^h(\omega), \quad (1)$$

is conveniently split in its hole (h) and particle (p) contribu-

^{a)}Corresponding author: loos@irsamc.ups-tlse.fr

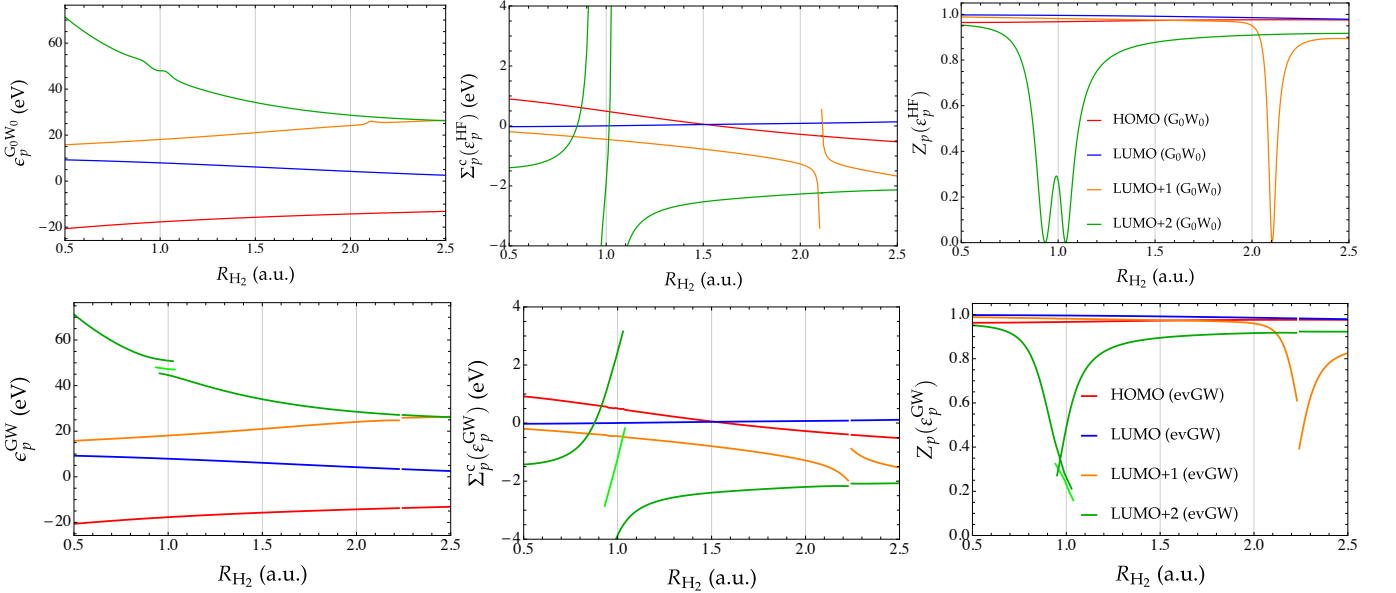


FIG. 1. QP energies (left), correlation part of the self-energy (center) and renormalization factor (right) as functions of the internuclear distance R_{H_2} for various orbitals of H_2 at the G_0W_0 @HF/6-31G (top) and $evGW$ @HF/6-31G (bottom) levels. For convenience, the intermediate (center) branch is presented in lighter green for the LUMO+2.

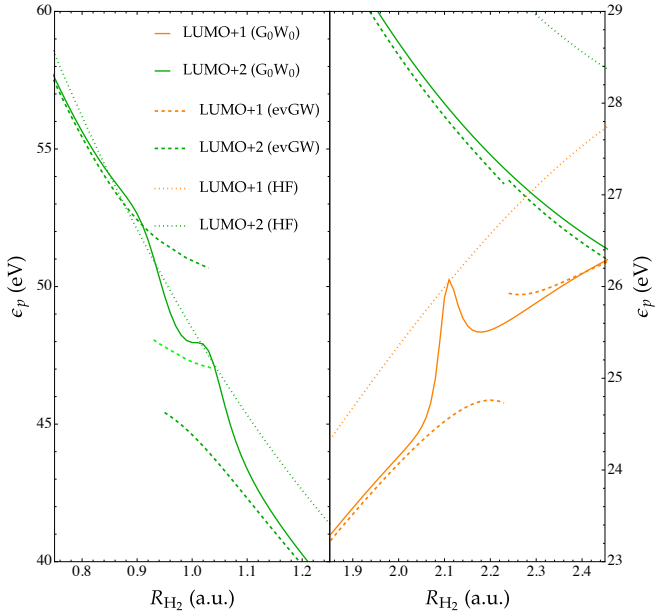


FIG. 2. HF orbital energies (dotted lines) and QP energies as functions of the internuclear distance R_{H_2} for the LUMO+1 and LUMO+2 orbitals of H_2 at the G_0W_0 @HF/6-31G (solid lines) and $evGW$ @HF/6-31G (dashed lines) levels. For convenience, the intermediate (center) branch is presented in lighter green for the LUMO+2.

tions

$$\Sigma_p^h(\omega) = 2 \sum_i^{\text{occ}} \sum_x \frac{[pi|x]^2}{\omega - \epsilon_i + \Omega_x - i\eta}, \quad (2a)$$

$$\Sigma_p^p(\omega) = 2 \sum_a^{\text{virt}} \sum_x \frac{[pa|x]^2}{\omega - \epsilon_a - \Omega_x + i\eta}, \quad (2b)$$

where η is a positive infinitesimal. The screened two-electron integrals

$$[pq|x] = \sum_{ia} (pq|ia)(\mathbf{X} + \mathbf{Y})_{ia}^x \quad (3)$$

are obtained via the contraction of the bare two-electron integrals⁶⁵ $(pq|rs)$ and the transition densities $(\mathbf{X} + \mathbf{Y})_{ia}^x$ originating from a random phase approximation (RPA) calculation^{66,67}

$$\begin{pmatrix} \mathbf{A} & \mathbf{B} \\ \mathbf{B} & \mathbf{A} \end{pmatrix} \begin{pmatrix} \mathbf{X} \\ \mathbf{Y} \end{pmatrix} = \mathbf{\Omega} \begin{pmatrix} \mathbf{1} & \mathbf{0} \\ \mathbf{0} & -\mathbf{1} \end{pmatrix} \begin{pmatrix} \mathbf{X} \\ \mathbf{Y} \end{pmatrix}, \quad (4)$$

with

$$A_{ia,jb} = \delta_{ij}\delta_{ab}(\epsilon_a - \epsilon_i) + 2(ia|jb), \quad B_{ia,jb} = 2(ia|bj), \quad (5)$$

and δ_{pq} is the Kronecker delta.⁶⁸ Equation (4) also provides the neutral excitation energies Ω_x .

In practice, there exist two ways of determining the G_0W_0 QP energies.^{5,6} In its “graphical” version, they are provided by one of the many solutions of the (non-linear) QP equation

$$\omega = \epsilon_p^{\text{HF}} + \text{Re}[\Sigma_p^c(\omega)]. \quad (6)$$

In this case, special care has to be taken in order to select the “right” solution, known as the QP solution. In particular, it

is usually worth calculating its renormalization weight (or factor), $Z_p(\epsilon_p^{\text{HF}})$, where

$$Z_p(\omega) = \left[1 - \frac{\partial \text{Re}[\Sigma_p^c(\omega)]}{\partial \omega} \right]^{-1}. \quad (7)$$

Because of sum rules,^{69–72} the other solutions, known as satellites, share the remaining weight. In a well-behaved case (belonging to the weakly correlated regime), the QP weight is much larger than the sum of the satellite weights, and of the order of 0.7–0.9.

Within the linearized version of G_0W_0 , one assumes that

$$\Sigma_p^c(\omega) \approx \Sigma_p^c(\epsilon_p^{\text{HF}}) + (\omega - \epsilon_p^{\text{HF}}) \frac{\partial \Sigma_p^c(\omega)}{\partial \omega} \Big|_{\omega=\epsilon_p^{\text{HF}}}, \quad (8)$$

that is, the self-energy behaves linearly in the vicinity of $\omega = \epsilon_p^{\text{HF}}$. Substituting (8) into (6) yields

$$\epsilon_p^{G_0W_0} = \epsilon_p^{\text{HF}} + Z_p(\epsilon_p^{\text{HF}}) \text{Re}[\Sigma_p^c(\epsilon_p^{\text{HF}})]. \quad (9)$$

Unless otherwise stated, in the remaining of this paper, the G_0W_0 QP energies are determined via the linearized method.

In the case of evGW, the QP energy, ϵ_p^{GW} , are obtained via Eq. (6), which has to be solved self-consistently due to the QP energy dependence of the self-energy [see Eq. (1)].^{11–14} At least in the weakly correlated regime where a clear QP solution exists, we believe that, within evGW, the self-consistent algorithm should select the solution of the QP equation (6) with the largest renormalization weight $Z_p(\epsilon_p^{\text{GW}})$. In order to avoid convergence issues, we have used the DIIS convergence accelerator technique proposed by Pulay.^{73,74} Moreover, throughout this paper, we have set $\eta = 0$.

III. RESULTS

A. Virtual orbitals

As a first example, we consider the hydrogen molecule H_2 in a relatively small gaussian basis set (6-31G) in order to be able to study easily the entire orbital energy spectrum. Although the number of irregularities/discontinuities as well as their locations may vary with the basis set, the conclusions we are going to draw here are general.

Figure 1 reports three key quantities as functions of the internuclear distance R_{H_2} for various orbitals at the G_0W_0 and the self-consistent evGW levels: i) the QP energies [$\epsilon_p^{G_0W_0}$ or ϵ_p^{GW}], ii) the correlation part of the self-energy [$\Sigma_p^c(\epsilon_p^{\text{HF}})$ or $\Sigma_p^c(\epsilon_p^{\text{GW}})$], and iii) the renormalization factor/weight [$Z_p(\epsilon_p^{\text{HF}})$ or $Z_p(\epsilon_p^{\text{GW}})$].

1. G_0W_0

Let us first consider the results of the G_0W_0 calculations reported in the top row of Fig. 1. Looking at the curves of

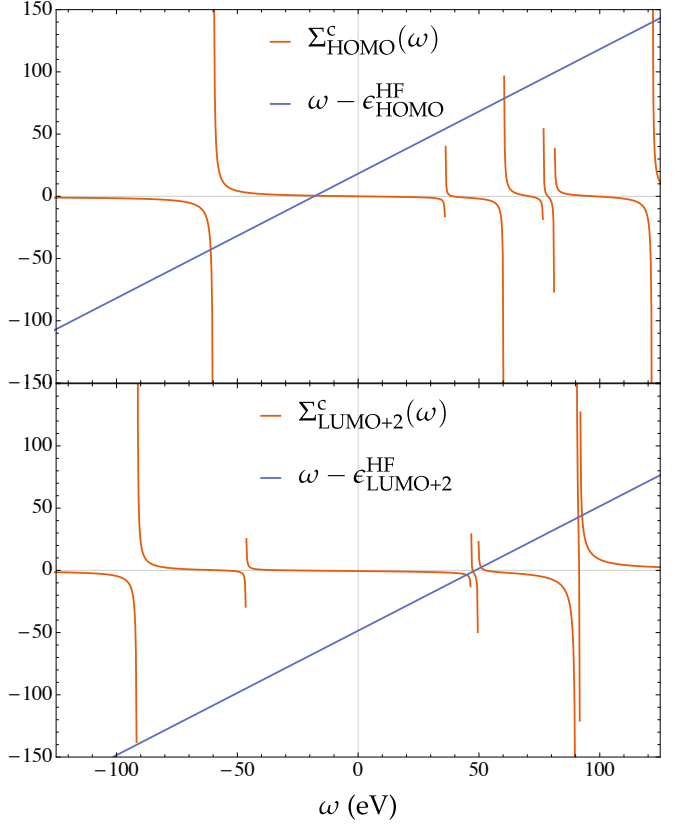


FIG. 3. $\Sigma_{\text{HOMO}}^c(\omega)$ and $\Sigma_{\text{LUMO}+2}^c(\omega)$ (in eV) as functions of the frequency ω obtained at the evGW@HF/6-31G level for H_2 at $R_{H_2} = 1.0$ bohr. The solutions of the QP equation are given by the intersection of the red and blue curves.

$\epsilon_p^{G_0W_0}$ as a function of R_{H_2} (top left graph of Fig. 1), one notices obvious irregularities in the LUMO+2 around $R_{H_2} = 1.0$ bohr and in the LUMO+1 around $R_{H_2} = 2.1$ bohr. For information, the experimental equilibrium geometry of H_2 is around $R_{H_2} = 1.4$ bohr.⁷⁵ These irregularities are unphysical, and occur in correspondence with a series of poles in $\Sigma_{\text{LUMO}+1}^c$ and $\Sigma_{\text{LUMO}+2}^c$ (see top center graph of Fig. 1). For example, one can notice two poles in $\Sigma_{\text{LUMO}+2}^c$ just before and after $R_{H_2} = 1.0$ bohr, giving birth to three branches. The origin of the irregularities in $\epsilon_{\text{LUMO}+1}$ and $\epsilon_{\text{LUMO}+2}$ can, therefore, be traced back to the wrong assumption that $\Sigma_{\text{LUMO}+1}^c(\omega)$ and $\Sigma_{\text{LUMO}+2}^c(\omega)$ are linear functions of ω in the vicinity of, respectively, $\omega = \epsilon_{\text{LUMO}+1}^{\text{HF}}$ and $\omega = \epsilon_{\text{LUMO}+2}^{\text{HF}}$ [see Eq. (8)].

However, despite the divergencies in the self-energy, the QP energies $\epsilon_{\text{LUMO}+1}^{G_0W_0}$ and $\epsilon_{\text{LUMO}+2}^{G_0W_0}$ remain finite thanks to a rapid decrease of the renormalization factor at the R_{H_2} values for which the self-energy diverges [see Eq. (6) and top right graph of Fig. 1]. For example, note that $Z_{\text{LUMO}+2}$ reaches exactly zero at the pole locations. A very similar scenario unfolds for the LUMO+1, except that a single pole is present in $\Sigma_{\text{LUMO}+1}^c$.

Let us analyze this point further. Since the self-energy behaves as $\Sigma_p^c \sim \delta^{-1}$ (with $\delta \rightarrow 0$) in the vicinity of a singularity, one can easily show that $Z_p \sim (1 + \delta^{-2})^{-1} \sim \delta^2$,

which yields $\epsilon_p^{G_0W_0} \sim \epsilon_p^{\text{HF}} + \delta$. In plain words, $\epsilon_p^{G_0W_0}$ remains finite near the poles of the self-energy thanks to the linearization of the QP equation [see Eq. (6)]. It also evidences that, at the pole locations (i.e. $\delta = 0$), we have $\epsilon_p^{G_0W_0} = \epsilon_p^{\text{HF}}$, i.e., by construction the QP energy is forced to remain equal to the zeroth-order energy. This is nicely illustrated in Fig. 2, where we have plotted the HF orbital energies (dotted lines) as well as the G_0W_0 QP energies (solid lines) around the two “problematic” internuclear distances. The behavior of $\epsilon_{\text{LUMO}+1}^{G_0W_0}$ (solid orange line on the right panel of Fig. 2) is particularly instructive and shows that the G_0W_0 QP energies can have an erratic behavior near the poles of the self-energy.

It is interesting to investigate further the origin of these poles. As evidenced by Eq. (1), for a calculation involving $2n$ electrons and N basis functions, the self-energy has exactly $nN(N - n)$ poles originating from the combination of the N poles of the Green function G (at frequencies ϵ_p) and the $n(N - n)$ poles of the screened Coulomb interaction W (at the RPA singlet excitations Ω_x). For example, at $R_{\text{H}_2} = 2.11$ bohr, the combination of $\epsilon_{\text{LUMO}}^{\text{HF}} = 3.83$ eV and the HOMO-LUMO-dominated first neutral excitation energy $\Omega_1 = 22.24$ eV are equal to the LUMO+1 energy $\epsilon_{\text{LUMO}+1}^{G_0W_0} = 26.07$ eV. Around $R_{\text{H}_2} = 1.0$ bohr, the two poles of $\Sigma_{\text{LUMO}+1}^c$ are due to the following accidental equalities: $\epsilon_{\text{LUMO}+1}^{G_0W_0} = \epsilon_{\text{LUMO}+1}^{\text{HF}} + \Omega_2$, and $\epsilon_{\text{LUMO}+1}^{G_0W_0} = \epsilon_{\text{LUMO}+1}^{\text{HF}} + \Omega_1$. Because the number of poles in G and W are both proportional to N , these spurious poles in the self-energy become more and more frequent for larger gaussian basis sets. For virtual orbitals, the higher in energy the orbital is, the earlier the singularities seem to appear.

Finally, the irregularities in the G_0W_0 QP energies as a function of R_{H_2} can also be understood as follows. Since within G_0W_0 only one pole of G is calculated, i.e., the QP energy, all the satellite poles are discarded. Mixing between QP and satellites poles, which is important when they are close to each other, hence, is not considered. This situation can be compared to the lack of mixing between single and double excitations in adiabatic time-dependent density-functional theory and the Bethe-Salpeter equation^{76–79} (see also Refs. 80–83).

2. evGW

Within partially self-consistent schemes, the presence of poles in the self-energy at a frequency similar to a QP energy has more dramatic consequences. The results for H_2 at the evGW@HF/6-31G level are reported in the bottom row of Fig. 1. Around $R_{\text{H}_2} = 1.0$ bohr, we observe that, for the LUMO+2, one can fall onto three distinct solutions depending on the algorithm one relies on to solve self-consistently the QP equation (see bottom left graph of Fig. 1). In order to obtain each of the three possible solutions in the vicinity of $R_{\text{H}_2} = 1.0$ bohr, we have run various sets of calculations using different starting values for the QP energies and sizes of the DIIS space. In particular, we clearly see that each of these solutions yield a distinct energy separated by several electron volts (see zoom in Fig. 2), and each of them is associated with a

well-defined branch of the self-energy, as shown by the center graph in the bottom row of Fig. 1. For convenience, the intermediate (center) branch is presented in lighter green in Figs. 1 and 2, while the left and right branches are depicted in darker green. Interestingly, the evGW iterations are able to “push” the QP solution away from the poles of the self-energy, which explains why the renormalization factor is never exactly equal to zero (see bottom right graph of Fig. 1). However, one cannot go smoothly from one branch to another, and each switch between solutions implies a significant energetic discontinuity. Moreover, we observe “ripple” effects in other virtual orbitals: a discontinuity in one of the QP energies induces (smaller) discontinuities in the others. This is a direct consequence of the global energy dependence of the self-energy [see Eq. (1)], and is evidenced on the left graph in the bottom row of Fig. 1 around $R_{\text{H}_2} = 2.1$ bohr.

The main observation of the present study is that each branch of the self-energy is associated with a distinct QP solution. We clearly see that, when one goes from one branch to another, there is a transfer of weight between the QP and one of the satellites, which becomes the QP on the new branch.⁴⁷ As opposed to the strongly correlated regime where the QP picture breaks down, i.e., there is no clear QP, here there is always a clear QP except at the vicinity of the poles where the weight transfer occurs. As for G_0W_0 , this sudden transfer is caused by the artificial removal of the satellite poles. However, in the evGW results the problem is amplified by the self-consistency. We expect that keeping the full frequency dependence of the self-energy would solve this problem.

It is also important to mention that the self-consistent algorithm is fairly robust as it rarely selects a solution with a renormalization weight lower than 0.5, as shown by the center graph in the bottom row of Fig. 1. In other words, when the renormalization factor of the QP solution becomes too small, the self-consistent algorithm switches naturally to a different solution. From a technical point of view, around the poles of the self-energy, it is particularly challenging to converge self-consistent calculations, and we heavily relied on DIIS to avoid such difficulties. We note that an alternative *ad hoc* approach to stabilize such self-consistent calculations is to increase the value of the positive infinitesimal η .

Figure 3 shows the correlation part of the self-energy for the HOMO and LUMO+2 orbitals as a function of ω (red curves) obtained at the self-consistent evGW@HF/6-31G level for H_2 with $R_{\text{H}_2} = 1.0$ bohr. The solutions of the QP equation (6) are given by the intersections of the red and blue curves. On the one hand, in the case of the HOMO, we have an unambiguous QP solution (at $\omega \approx -20$ eV) which is well separated from the other solutions. In this case, one can anticipate a large value of the renormalization factor Z_{HOMO} as the self-energy is flat around the intersection of the two curves. On the other hand, for the LUMO+2, we see three solutions of the QP equation very close in energy from each other around $\omega = 50$ eV. In this particular case, there is no well-defined QP peak as each solution has a fairly small weight. Therefore, one may anticipate multiple solution issues when a solution of the QP equation is close to a pole of the self-energy.

Finally, we note that the multiple solutions discussed here

are those of the QP equation, i.e., *multiple* QP poles associated to a *single* Green function. This is different from the multiple solutions discussed in Refs. 84–90, in which it is shown that, in general, the nonlinear Dyson equation admits *multiple* Green functions, which can be physical but also unphysical.

B. Occupied orbitals

So far, we have seen that multiple solutions seem to only appear for virtual orbitals (LUMO excluded). However, we will show here that it can also happen in occupied orbitals. We take as an example the fluorine molecule (F_2) in a minimal basis set (STO-3G), and perform evGW@HF calculations within the frozen-core approximation, that is, we do not update the orbital energies associated with the core orbitals. Figure 4 shows the behavior (as a function of the distance between the two fluorine atoms R_{F_2}) of the same quantities as in Fig. 1 but for some of the occupied orbitals of F_2 (HOMO-6, HOMO-5 and HOMO-4). Similarly to the case of H_2 discussed in the previous section, we see discontinuities in the QP energies around $R_{F_2} = 2.3$ bohr (for the HOMO-6) and $R_{F_2} = 2.7$ bohr (for the HOMO-5). For information, the experimental equilibrium geometry of F_2 is $R_{F_2} = 2.668$ bohr, which evidences that the second discontinuity is extremely close to the experimental geometry. Let us mention here that we have not found any discontinuity in the HOMO orbital. The case of the frontier orbitals will be discussed below. For F_2 , here again, we clearly observe ripple effects on other occupied orbitals. Similarly to virtual orbitals, we have found that the lower in energy the orbital is, the earlier the singularities seem to appear.

C. Frontier orbitals

Before concluding, we would like to know, whether or not, this multisolution behavior can potentially appear in frontier orbitals. This is an important point to discuss as these orbitals are directly related to the ionization potential and the electron affinity, hence to the gap.

Let us take the HOMO orbital as an example. A similar rationale holds for the LUMO orbital. According to the expression of the hole and particle parts of the self-energy given in Eqs. (2a) and (2b) respectively, $\Sigma_{\text{HOMO}}^c(\omega)$ has poles at $\omega = \epsilon_i - \Omega_x$ and $\omega = \epsilon_a + \Omega_x$ with $\Omega_x > 0$. Evaluating the self-energy at $\omega = \epsilon_{\text{HOMO}}$ would yield $\epsilon_{\text{HOMO}} - \epsilon_i = -\Omega_x$ and $\epsilon_{\text{HOMO}} - \epsilon_a = +\Omega_x$, which is in clear contradiction with the assumption that $\Omega_x > 0$. Therefore, the self-energy is never singular at $\omega = \epsilon_{\text{HOMO}}$ and $\omega = \epsilon_{\text{LUMO}}$ and the linearized G_0W_0 equations can be solved without any problem for the frontier orbitals. This is true for any G_0 , that is, it does not depend on the starting point. As can be seen from Eqs. (2a) and (2b), the two poles of the self-energy closest to the Fermi level are located at $\omega = \epsilon_{\text{HOMO}} - \Omega_1$ and $\omega = \epsilon_{\text{LUMO}} + \Omega_1$. As a consequence, there is a region equal to $\epsilon_{\text{HOMO}} - \epsilon_{\text{LUMO}} + 2\Omega_1$ around the Fermi level in which the self-energy does not have

poles. Because $\Omega_1 \approx \epsilon_{\text{HOMO}} - \epsilon_{\text{LUMO}} = E_{\text{gap}}$, this region is approximately equal to $3E_{\text{gap}}$.

For “graphical” G_0W_0 , the solution might lie outside this range, even for the frontier orbitals. This can happen when E_{gap} is much smaller than the true GW gap. In particular, this could occur for graphical G_0W_0 on top of a Kohn-Sham starting point, which is known to yield gaps that are (much) smaller than GW gaps. Within graphical G_0W_0 , multiple solution issues for the HOMO have been reported by van Setten and coworkers^{9,34} in several systems (LiH, BN, BeO and O₃). In their calculations, they employed PBE orbital energies⁹¹ as starting point, and this type of functionals is well known to drastically underestimate E_{gap} .⁹²

As an example, we have computed, within the frozen-core approximation, $\Sigma_{\text{HOMO}}^c(\omega)$ and $\Sigma_{\text{LUMO}}^c(\omega)$ as functions of ω at the $G_0W_0@\text{PBE/cc-pVDZ}$ level for beryllium monoxide (BeO) at its experimental geometry (i.e. $R_{\text{BeO}} = 2.515$ bohr).⁷⁵ These calculations have been performed with MOLGW.³¹ The results are gathered in Fig. 5, where one clearly sees that multiple solutions appear for both the HOMO and LUMO orbitals. Note that performing the same set of calculations with a HF starting point yields a perfectly unambiguous single QP solution. For this system, PBE is a particularly bad starting point for a GW calculation with a HOMO-LUMO gap equal to 1.35 eV. Using the same basis set, HF yields a gap of 8.96 eV, while $G_0W_0@\text{HF}$ and $G_0W_0@\text{PBE}$ yields 7.54 and 5.60 eV. The same observations can be made for the other systems reported as problematic by van Setten and coworkers.^{9,34} As a general rule, it is known that HF is usually a better starting point for GW in small molecular systems.^{8,13,47,93} For larger systems, hybrid functionals⁹⁴ might be the ideal compromise, thanks to the increase of the HOMO-LUMO gap via the addition of (exact) HF exchange.^{8,35,38,46,95}

IV. CONCLUDING REMARKS

The GW approximation of many-body perturbation theory has been highly successful at predicting the electronic properties of solids and molecules.^{2–4} However, it is also known to be inadequate to model strongly correlated systems.^{87,96–99} Here, we have found severe shortcomings of two widely-used variants of GW in the weakly correlated regime. We have evidenced that one can hit multiple solution issues within G_0W_0 and evGW due to the location of the QP solution near poles of the self-energy. Within linearized G_0W_0 , this implies irregularities in key experimentally-measurable quantities of simple diatomics, while, at the partially self-consistent evGW level, discontinuities arise. Because the RPA correlation energy^{31,66,100,101} and the Bethe-Salpeter excitation energies^{30,102,103} directly dependent on the QP energies, these types of discontinuities are also present in these quantities, hence in the energy surfaces of ground and excited states. Illustrative examples can be found in our previous study.⁴⁷ We believe that such discontinuities would not exist within a fully self-consistent scheme where one takes into account the QP peak as well as its satellites at each iteration. Obviously, this latter point deserves further investigations. However,

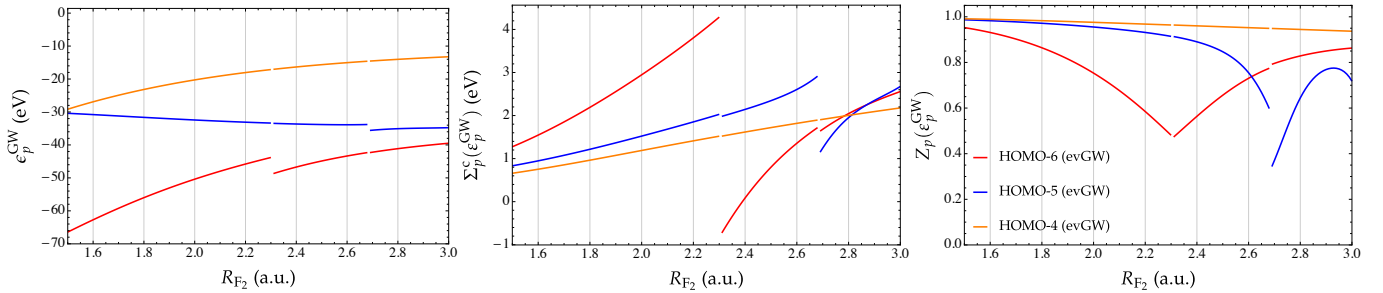


FIG. 4. QP energies (left), correlation part of the self-energy (center) and renormalization factor (right) as functions of the internuclear R_{F_2} for various occupied orbitals of F_2 at the evGW@HF/STO-3G level.

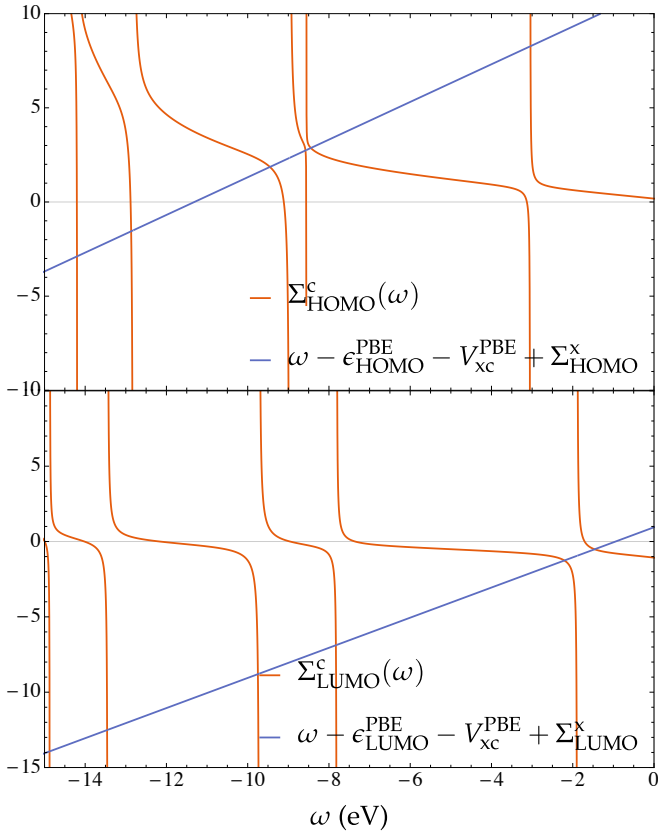


FIG. 5. $\Sigma_{HOMO}^c(\omega)$ and $\Sigma_{LUMO}^c(\omega)$ (in eV) as functions of the frequency ω obtained at the G_0W_0 @PBE/cc-pVDZ level for BeO at its experimental geometry.⁷⁵ The solutions of the QP equations are given by the intersection of the red and blue curves.

if confirmed, this would be a strong argument in favor of fully self-consistent schemes. Also, for extended systems, these issues might be mitigated by the plasmon modes that dominate the high-energy spectrum of the screened Coulomb interaction. We are currently exploring different routes in order to remove these unphysical features. Padé resummation technique could be of great interest¹⁰⁴ for such purpose.

ACKNOWLEDGMENTS

PFL would like to thank Xavier Blase and Fabien Bruneval for valuable discussions. The authors would like to thank Valerio Olevano for stimulating discussions during his sabbatical stay at IRSAMC. MV thanks *Université Paul Sabatier* (Toulouse, France) for a PhD scholarship.

- ¹L. Hedin, Phys. Rev. **139**, A796 (1965).
- ²G. Onida, L. Reining, and A. R. and, Rev. Mod. Phys. **74**, 601 (2002).
- ³F. Aryasetiawan and O. Gunnarsson, Rep. Prog. Phys. **61**, 237 (1998).
- ⁴L. Reining, Wiley Interdiscip. Rev. Comput. Mol. Sci. , e1344 (2017).
- ⁵M. S. Hybertsen and S. G. Louie, Phys. Rev. Lett. **55**, 1418 (1985).
- ⁶M. J. van Setten, F. Weigend, and F. Evers, J. Chem. Theory Comput. **9**, 232 (2013).
- ⁷F. Bruneval, J. Chem. Phys. **136**, 194107 (2012).
- ⁸F. Bruneval and M. A. L. Marques, J. Chem. Theory Comput. **9**, 324 (2013).
- ⁹M. J. van Setten, F. Caruso, S. Sharifzadeh, X. Ren, M. Scheffler, F. Liu, J. Lischner, L. Lin, J. R. Deslippe, S. G. Louie, C. Yang, F. Weigend, J. B. Neaton, F. Evers, and P. Rinke, J. Chem. Theory Comput. **11**, 5665 (2015).
- ¹⁰M. J. van Setten, R. Costa, F. Vines, and F. Illas, J. Chem. Theory Comput. **14**, 877 (2018).
- ¹¹M. S. Hybertsen and S. G. Louie, Phys. Rev. B **34**, 5390 (1986).
- ¹²M. Shishkin and G. Kresse, Phys. Rev. B **75**, 235102 (2007).
- ¹³X. Blase, C. Attaccalite, and V. Olevano, Phys. Rev. B **83**, 115103 (2011).
- ¹⁴C. Faber, C. Attaccalite, V. Olevano, E. Runge, and X. Blase, Phys. Rev. B **83**, 115123 (2011).
- ¹⁵S. V. Faleev, M. van Schilfgaarde, and T. Kotani, Phys. Rev. Lett. **93**, 126406 (2004).
- ¹⁶M. van Schilfgaarde, T. Kotani, and S. Faleev, Phys. Rev. Lett. **96**, 226402 (2006).
- ¹⁷T. Kotani, M. van Schilfgaarde, and S. V. Faleev, Phys. Rev. B **76**, 165106 (2007).
- ¹⁸S.-H. Ke, Phys. Rev. B **84**, 205415 (2011).
- ¹⁹F. Kaplan, M. E. Harding, C. Seiler, F. Weigend, F. Evers, and M. J. van Setten, J. Chem. Theory Comput. **12**, 2528 (2016).
- ²⁰A. Stan, N. E. Dahlen, and R. van Leeuwen, Europhys. Lett. **76**, 298 (2006).
- ²¹A. Stan, N. E. Dahlen, and R. van Leeuwen, J. Chem. Phys. **130**, 114105 (2009).
- ²²C. Rostgaard, K. W. Jacobsen, and K. S. Thygesen, Phys. Rev. B **81**, 085103 (2010).
- ²³F. Caruso, P. Rinke, X. Ren, M. Scheffler, and A. Rubio, Phys. Rev. B **86**, 081102(R) (2012).
- ²⁴F. Caruso, D. R. Rohr, M. Hellgren, X. Ren, P. Rinke, A. Rubio, and M. Scheffler, Phys. Rev. Lett. **110**, 146403 (2013).
- ²⁵F. Caruso, P. Rinke, X. Ren, A. Rubio, and M. Scheffler, Phys. Rev. B **88**, 075105 (2013).
- ²⁶F. Caruso, *Self-Consistent GW Approach for the Unified Description of Ground and Excited States of Finite Systems*, PhD Thesis, Freie Universität Berlin (2013).

²⁷P. Koval, D. Foerster, and D. Sánchez-Portal, *Phys. Rev. B* **89**, 155417 (2014).

²⁸J. Wilhelm, D. Golze, L. Talirz, J. Hutter, and C. A. Pignedoli, *J. Phys. Chem. Lett.* **9**, 306 (2018).

²⁹F. Caruso, M. Dauth, M. J. van Setten, and P. Rinke, *J. Chem. Theory Comput.* **12**, 5076 (2016).

³⁰X. Blase, I. Duchemin, and D. Jacquemin, *Chem. Soc. Rev.* **47**, 1022 (2018).

³¹F. Bruneval, T. Rangel, S. M. Hamed, M. Shao, C. Yang, and J. B. Neaton, *Comput. Phys. Commun.* **208**, 149 (2016).

³²F. Kaplan, F. Weigend, F. Evers, and M. J. van Setten, *J. Chem. Theory Comput.* **11**, 5152 (2015).

³³K. Krause and W. Klopper, *J. Comput. Chem.* **38**, 383 (2017).

³⁴E. Maggio, P. Liu, M. J. van Setten, and G. Kresse, *J. Chem. Theory Comput.* **13**, 635 (2017).

³⁵F. Bruneval, S. M. Hamed, and J. B. Neaton, *J. Chem. Phys.* **142**, 244101 (2015).

³⁶F. Bruneval, *J. Chem. Phys.* **145**, 234110 (2016).

³⁷L. Hung, F. H. da Jornada, J. Souto-Casares, J. R. Chelikowsky, S. G. Louie, and S. Öğüt, *Phys. Rev. B* **94**, 085125 (2016).

³⁸P. Boulanger, D. Jacquemin, I. Duchemin, and X. Blase, *J. Chem. Theory Comput.* **10**, 1212 (2014).

³⁹D. Jacquemin, I. Duchemin, A. Blondel, and X. Blase, *J. Chem. Theory Comput.* **13**, 767 (2017).

⁴⁰J. Li, M. Holzmann, I. Duchemin, X. Blase, and V. Olevano, *Phys. Rev. Lett.* **118**, 163001 (2017).

⁴¹L. Hung, F. Bruneval, K. Baishya, and S. Öğüt, *J. Chem. Theory Comput.* **13**, 2135 (2017).

⁴²R. M. Richard, M. S. Marshall, O. Dolgounitcheva, J. V. Ortiz, J.-L. Brédas, N. Marom, and C. D. Sherrill, *J. Chem. Theory Comput.* **12**, 595 (2016).

⁴³L. Gallandi, N. Marom, P. Rinke, and T. Körzdörfer, *J. Chem. Theory Comput.* **12**, 605 (2016).

⁴⁴J. W. Knight, X. Wang, L. Gallandi, O. Dolgounitcheva, X. Ren, J. V. Ortiz, P. Rinke, T. Körzdörfer, and N. Marom, *J. Chem. Theory Comput.* **12**, 615 (2016).

⁴⁵O. Dolgounitcheva, M. Díaz-Tinoco, V. G. Zakrzewski, R. M. Richard, N. Marom, C. D. Sherrill, and J. V. Ortiz, *J. Chem. Theory Comput.* **12**, 627 (2016).

⁴⁶D. Jacquemin, I. Duchemin, and X. Blase, *J. Chem. Theory Comput.* **11**, 3290 (2015).

⁴⁷P. F. Loos, P. Romaniello, and J. A. Berger, *J. Chem. Theory Comput.* **14**, 3071 (2018).

⁴⁸M. Seidl, *Phys. Rev. A* **75**, 062506 (2007).

⁴⁹P.-F. Loos and P. M. W. Gill, *Phys. Rev. A* **79**, 062517 (2009).

⁵⁰P.-F. Loos and P. M. W. Gill, *Phys. Rev. Lett.* **103**, 123008 (2009).

⁵¹P.-F. Loos and P. M. Gill, *Mol. Phys.* **108**, 2527 (2010).

⁵²P.-F. Loos and P. M. W. Gill, *J. Chem. Phys.* **135**, 214111 (2011).

⁵³P. M. W. Gill and P.-F. Loos, *Theor. Chem. Acc.* **131**, 1069 (2012).

⁵⁴A. Szabo and N. S. Ostlund, *Modern quantum chemistry* (McGraw-Hill, New York, 1989).

⁵⁵M. E. Casida and D. P. Chong, *Phys. Rev. A* **40**, 4837 (1989).

⁵⁶M. E. Casida and D. P. Chong, *Phys. Rev. A* **44**, 5773 (1991).

⁵⁷G. Stefanucci and R. van Leeuwen, *Nonequilibrium Many-Body Theory of Quantum Systems: A Modern Introduction* (Cambridge University Press, Cambridge, 2013).

⁵⁸J. V. Ortiz, *Wiley Interdiscip. Rev. Comput. Mol. Sci.* **3**, 123 (2013).

⁵⁹J. J. Phillips and D. Zgid, *J. Chem. Phys.* **140**, 241101 (2014).

⁶⁰J. J. Phillips, A. A. Kananenka, and D. Zgid, *J. Chem. Phys.* **142**, 194108 (2015).

⁶¹A. A. Rusakov, J. J. Phillips, and D. Zgid, *J. Chem. Phys.* **141**, 194105 (2014).

⁶²A. A. Rusakov and D. Zgid, *J. Chem. Phys.* **144**, 054106 (2016).

⁶³S. Hirata, M. R. Hermes, J. Simons, and J. V. Ortiz, *J. Chem. Theory Comput.* **11**, 1595 (2015).

⁶⁴S. Hirata, A. E. Doran, P. J. Knowles, and J. V. Ortiz, *J. Chem. Phys.* **147**, 044108 (2017).

⁶⁵P. M. W. Gill, *Adv. Quantum Chem.* **25**, 141 (1994).

⁶⁶M. E. Casida, *Phys. Rev. A* **51**, 2005 (1995).

⁶⁷A. Dreuw and M. Head-Gordon, *Chem. Rev.* **105**, 4009 (2005).

⁶⁸F. W. J. Olver, D. W. Lozier, R. F. Boisvert, and C. W. Clark, eds., *NIST Handbook of Mathematical Functions* (Cambridge University Press, New York, 2010).

⁶⁹P. C. Martin and J. Schwinger, *Phys. Rev.* **115**, 1342 (1959).

⁷⁰G. Baym and L. P. Kadanoff, *Phys. Rev.* **124**, 287 (1961).

⁷¹G. Baym, *Phys. Rev.* **127**, 1391 (1962).

⁷²U. von Barth and B. Holm, *Phys. Rev. B* **54**, 8411 (1996).

⁷³P. Pulay, *Chem. Phys. Lett.* **73**, 393 (1980).

⁷⁴P. Pulay, *J. Comput. Chem.* **3**, 556 (1982).

⁷⁵K. P. Huber and G. Herzberg, *Molecular Spectra and Molecular Structure: IV. Constants of diatomic molecules* (van Nostrand Reinhold Company, 1979).

⁷⁶N. T. Maitra, R. J. C. F. Zhang, and K. Burke, *J. Chem. Phys.* **120**, 5932 (2004).

⁷⁷R. J. Cave, F. Zhang, N. T. Maitra, and K. Burke, *Chem. Phys. Lett.* **389**, 39 (2004).

⁷⁸P. Romaniello, D. Sangalli, J. A. Berger, F. Sottile, L. G. Molinari, L. Reining, and G. Onida, *J. Chem. Phys.* **130**, 044108 (2009).

⁷⁹D. Sangalli, P. Romaniello, G. Onida, and A. Marini, *J. Chem. Phys.* **134**, 034115 (2011).

⁸⁰Z. Li, B. Suo, and W. Liu, *J. Chem. Phys.* **141**, 244105 (2014).

⁸¹Q. Ou, G. D. Bellchambers, F. Furche, and J. E. Subotnik, *J. Chem. Phys.* **142**, 064114 (2015).

⁸²X. Zhang and J. M. Herbert, *J. Chem. Phys.* **142**, 064109 (2015).

⁸³S. M. Parker, S. Roy, and F. Furche, *The Journal of Chemical Physics* **145**, 134105 (2016).

⁸⁴E. Kozik, M. Ferrero, and A. Georges, *Phys. Rev. Lett.* **114**, 156402 (2015).

⁸⁵A. Stan, P. Romaniello, S. Rigamonti, L. Reining, and J. A. Berger, *New J. Phys.* **17**, 093045 (2015).

⁸⁶R. Rossi and F. Werner, *J. Phys. A: Math. Theor.* **48**, 485202 (2015).

⁸⁷W. Tarantino, P. Romaniello, J. A. Berger, and L. Reining, *Phys. Rev. B* **96**, 045124 (2017).

⁸⁸T. Schäfer, G. Rohringer, O. Gunnarsson, S. Ciuchi, G. Sangiovanni, and A. Toschi, *Phys. Rev. Lett.* **110**, 246405 (2013).

⁸⁹T. Schäfer, S. Ciuchi, M. Wallerberger, P. Thunström, O. Gunnarsson, G. Sangiovanni, G. Rohringer, and A. Toschi, *Phys. Rev. B* **94**, 235108 (2016).

⁹⁰O. Gunnarsson, G. Rohringer, T. Schäfer, G. Sangiovanni, and A. Toschi, *Phys. Rev. Lett.* **119**, 056402 (2017).

⁹¹J. P. Perdew, K. Burke, and M. Ernzerhof, *Phys. Rev. Lett.* **77**, 3865 (1996).

⁹²R. G. Parr and W. Yang, *Density-functional theory of atoms and molecules* (Oxford, Clarendon Press, 1989).

⁹³M. F. Lange and T. C. Berkelbach, arXiv, 1805.00043 (2018).

⁹⁴A. D. Becke, *J. Chem. Phys.* **98**, 5648 (1993).

⁹⁵X. Gui, C. Holzer, and W. Klopper, *J. Chem. Theory Comput.* **14**, 2127 (2018).

⁹⁶P. Romaniello, S. Guyot, and L. Reining, *J. Chem. Phys.* **131**, 154111 (2009).

⁹⁷P. Romaniello, F. Bechstedt, and L. Reining, *Phys. Rev. B* **85**, 155131 (2012).

⁹⁸S. Di Sabatino, J. A. Berger, L. Reining, and P. Romaniello, *J. Chem. Phys.* **143**, 024108 (2015).

⁹⁹S. Di Sabatino, J. A. Berger, L. Reining, and P. Romaniello, *Physical Review B* **94**, 155141 (2016).

¹⁰⁰N. E. Dahlen, R. van Leeuwen, and U. von Barth, *Phys. Rev. A* **73**, 012511 (2006).

¹⁰¹F. Furche, *J. Chem. Phys.* **129**, 114105 (2008).

¹⁰²G. Strinati, *Riv. Nuovo Cimento* **11**, 1 (1988).

¹⁰³X. Leng, F. Jin, M. Wei, and Y. Ma, *Wiley Interdiscip. Rev. Comput. Mol. Sci.* **6**, 532 (2016).

¹⁰⁴Y. Pavlyukh, *Nature* **7**, 504 (2017).